The Effects of Benoxacor on the Liver and Gut Microbiome of C57BL/6 Mice

Derek Simonsen,[*,†,‡] Nicole Cady,[§] Chunyun Zhang,[*] Rachel L. Shrode,[¶] Michael L. McCormick,[‖] Douglas R. Spitz [ID],[‖] Michael S. Chimenti,[‖‖] Kai Wang,[**] Ashutosh Mangalam,[§] and Hans-Joachim Lehmler [ID][*,†,‡,1]

[*]Department of Occupational and Environmental Health, The University of Iowa, Iowa City, Iowa 52242, USA; [†]Interdisciplinary Graduate Program in Human Toxicology, The University of Iowa, Iowa City, Iowa 52242, USA; [‡]IIHR Hydroscience and Engineering, The University of Iowa, Iowa City, Iowa 52242, USA; [§]Department of Pathology, The University of Iowa, Iowa City, Iowa 52242, USA; [¶]Department of Informatics, The University of Iowa, Iowa City, Iowa 52242, USA [‖]Free Radical and Radiation Biology Program, Department of Radiation Oncology, The University of Iowa, Iowa City, Iowa 52242, USA; [‖‖]Iowa Institute of Human Genetics, Carver College of Medicine, The University of Iowa, Iowa City, Iowa 52242, USA; and [**]Department of Biostatistics, The University of Iowa, Iowa City, Iowa 52242, USA

[1]To whom correspondence should be addressed at Department of Occupational and Environmental Health, The University of Iowa, University of Iowa Research Park, #164 MTF, Iowa City, IA 52242-5000, USA. E-mail: hans-joachim-lehmler@uiowa.edu.

ABSTRACT

The toxicity of many "inert" ingredients of pesticide formulations, such as safeners, is poorly characterized, despite evidence that humans may be exposed to these chemicals. Analysis of ToxCast data for dichloroacetamide safeners with the ToxPi tool identified benoxacor as the safener with the highest potential for toxicity, especially liver toxicity. Benoxacor was subsequently administered to mice via oral gavage for 3 days at concentrations of 0, 0.5, 5, and 50 mg/kg bodyweight (b.w.). Bodyweight-adjusted liver and testes weights were significantly increased in the 50 mg/kg b.w. group. There were no overt pathologies in either the liver or the intestine. 16S rRNA analysis of the cecal microbiome revealed no effects of benoxacor on α- or β-diversity; however, changes were observed in the abundance of certain bacteria. RNAseq analysis identified 163 hepatic genes affected by benoxacor exposure. Benoxacor exposure expressed a gene regulation profile similar to dichloroacetic acid and the fungicide sedaxane. Metabolomic analysis identified 9 serum and 15 liver metabolites that were affected by benoxacor exposure, changes that were not significant after correcting for multiple comparisons. The activity of antioxidant enzymes was not altered by benoxacor exposure. *In vitro* metabolism studies with liver microsomes and cytosol from male mice demonstrated that benoxacor is enantioselectively metabolized by cytochrome P450 enzymes, carboxylesterases, and glutathione S-transferases. These findings suggest that the minor toxic effects of benoxacor may be due to its rapid metabolism to toxic metabolites, such as dichloroacetic acid. This result challenges the assumption that inert ingredients of pesticide formulations are safe.

Key words: agrochemicals; biotransformation; chiral; dose response; environmental chemicals; exposure, environmental.

Reducing the potential health risks associated with agricultural pesticide use is critical as modern agriculture utilizes approximately 2 million tons of pesticides annually to enhance crop yields (Sharma et al., 2019). Globally, approximately $40 billion is spent on the application of pesticides each year, which leads to a 4- to 5-fold return on investment for farmers in developed countries (Gianessi and Reigner, 2007; Popp et al., 2013). However, the widespread use of pesticides has led to environmental contamination, raising concerns about possible human exposure to pesticides through surface and groundwater (Lari et al., 2014; Reemtsma et al., 2013; Wauchope, 1978) or diet (Carvalho, 2017; Reeves et al., 2019). For example, the herbicide metolachlor was detected in surface water in different agricultural watersheds across the United States (Rose et al., 2018). Metolachlor was also found in surface waters from Ontario (Canada) (Byer et al., 2011) and Southwestern France (Roubeix et al., 2012). In addition to the actual pesticide, commercial pesticide formulations contain ingredients, such as surfactants, solvents, and preservatives that ensure the product's effectiveness against the target pest (Cox and Surgan, 2006). Identifying these inert ingredients on product labels is not required in the United States, even though inert ingredients on average account for 86% of the total formulation (Surgan et al., 2010).

The U.S. government has regulated the production and use of pesticides, such as metolachlor, with the Federal Insecticide, Fungicide, and Rodenticide Act (FIFRA) to minimize the adverse effects of pesticides on the environment and human health (Bergeson, 2000). Under FIFRA, pesticides are regulated by the U.S. Environmental Protection Agency (EPA) (Gray, 2002). However, these regulations only cover the active ingredients of herbicide formulations. All other constituents of pesticide formulations are considered "inert" from a regulatory perspective because they do not have biological activity against a pest. As a consequence, the inert ingredients are not held to the same regulatory standards (Sivey et al., 2015). For example, the registration of pesticide formulations requires only 7 toxicological tests compared with 20 tests needed to register pesticides (Cox and Surgan, 2006). Importantly, pesticide applicators, including farmers, and the general public, often believe that these "inert" ingredients have no potential toxicities (Cox and Surgan, 2006). However, a growing number of toxic outcomes are associated with inert ingredients in the literature, including cardiovascular issues (Koyama et al., 1997), mitochondrial dysfunction (Oakes and Pollak, 1999), and genotoxicity (Bolognesi et al., 1997).

Herbicide safeners, such as benoxacor, are a class of inactive ingredients. They are often coformulated with the chloroacetanilide herbicides, for example, metolachlor (Su et al., 2019), to protect the target crop from the toxicity of the herbicide. Like metolachlor, these safeners have been detected seasonally in surface waters at concentrations ranging from 4 to 190 ng/l (Woodward et al., 2018), thus raising concerns of human coexposures to herbicides and the coformulated safeners. Unlike metolachlor, the potential toxicity of these safeners has received little attention. Limited in vitro data for several safeners are available in the ToxCast database. This database was created by the EPA for prioritizing chemicals with the greatest human health hazards through high-throughput screening, computational chemistry, and toxicogenomic technologies (Dix et al., 2007). Some toxicity information on benoxacor is also available through the European Chemical Agency (ECHA). These studies suggest that benoxacor has limited oral and inhalation toxicity following acute exposure. For example, the acute LD_{50}

values were > 5000 mg/kg b.w., > 5000 mg/kg b.w., and > 2010 mg/kg b.w. in acute oral and inhalation studies in rats and dermal exposure in rabbits, respectively.

We used ToxCast data to compare potential mechanisms by which current use safeners may cause toxicity and identify a safener for further toxicological studies. This analysis identified benoxacor as the safener with the most potential for toxicity, with hepatotoxicity being the primary endpoint of concern. We subsequently used a systems biology approach to assess the toxicity of benoxacor in male mice following subacute oral exposure and characterized the host metabolism of benoxacor in vitro. Our results demonstrate that high throughput screening data, combined with in vitro metabolism studies, likely have more potential to predict the toxicity of current use inert ingredients in vivo and, thus, enable the assessment of risks associated with these widely used agrochemicals.

MATERIALS AND METHODS

Chemicals and preparation of benoxacor solutions. Benoxacor (purity $\geq 97\%$; InChIKey: ZSDSQXJSNMTJDA-UHFFFAOYSA-N) was purchased as a brown solid from Accel Pharmtech (East Brunswick, New Jersey). Acenaphthene (99.3% purity; InChIKey: CWRYPZZKDGJXCA-UHFFFAOYSA-N; internal standard) was obtained from Accustandard (New Haven, Connecticut). Trifluralin (99.3% purity; InChIKey: PFJJMJDEVDLPNE-UHFFFAOYSA-N; recovery standard) was provided by Sigma-Aldrich (St. Louis, Missouri). ACS grade chemicals ($\geq 98\%$ purity) for in vitro buffer preparation were obtained from commercial sources. Pooled microsomal (catalog number M5000, lot number 1810172) and cytosolic (catalog number M5000.C, lot number 151032) preparations from C57Bl/6 male mouse livers ($n = 400$) were purchased from Sekisui XenoTech (Lenexa, Kansas). Nicotinamide adenine dinucleotide phosphate (NADPH) tetrasodium salt (lot number 3207105) was purchased from EMD Millipore Sigma (Temecula, California). Reduced glutathione (lot number SLCF3302) was procured from Sigma-Aldrich. Pesticide grade ethyl acetate was purchased from Fisher Chemical (Fair Lawn, New Jersey) for benoxacor extraction. Corn oil from Fisher Chemical was used to make benoxacor dosing solutions.

Analysis of ToxCast data for herbicide safeners. ToxCast data were compiled from the ToxCast Screening Library of the EPA (EPA, nd). All activity concentration (AC_{50}) values for the dichloroacetamide safeners benoxacor, AD-67, and dichlormid; the coformulated chloroacetanilide herbicides metolachlor, acetochlor, and alachlor; dichloroacetic acid, a likely metabolite of benoxacor; and for 2 structurally different current-use pesticides, 2,4-D and dicamba were scaled from 0 to 1 using equation 1, as previously described (Marvel et al., 2018):

$$\text{Scaled } AC_{50} = 1 - \left(\frac{(AC_{50} - AC_{50 \text{ minimum})}}{(AC_{50 \text{ maximum}} - AC_{50 \text{ minimum}})} \right). \quad (1)$$

Tests were categorized into groups (slices) according to the intended target family classification provided in ToxCast. The area of each slice was set to be proportional to the relative value of the chemical's bioactivity within the dataset. We then used the ToxPi hierarchical clustering feature to determine how benoxacor clustered with structurally similar herbicides with known toxicities (eg, metolachlor, acetochlor, or alachlor) or structurally unrelated herbicides (ie, 2,4-D and dicamba).

Animals and benoxacor exposure. Thirty-two 4-week-old male C57BL/6J mice were purchased from the Jackson Laboratory (Bar Harbor, Maine). Animals were acclimated to the animal facility at the University of Iowa for 4 weeks. On week 4, animals were transferred to fresh cages, soiled bedding was mixed and distributed among the new cages to normalize the microbiota across all animals before benoxacor exposure. At the beginning of the benoxacor exposure, cages had no statistically significant bodyweight difference (bodyweight range 20.7–28 g). The mice were maintained on a 12/12 h light/dark cycle and provided standard rodent chow (Envigo 7013, Envigo, Madison, Wisconsin) and water *ad libitum*. Animals were randomly assigned to cages with the random number function of MS Excel 2016.

Mice were exposed for 3 consecutive days between 9 and 11 AM to corn oil (PO, 10 ml/kg b.w.) or to benoxacor in corn oil for a final dose (PO, 0.5, 5, or 50 mg/kg b.w.). Similar dosing regimens are often used to study the dose-dependent effects of xenobiotics on hepatic drug-metabolizing enzyme gene expression (Cheng *et al.*, 2018; Li *et al.*, 2017). The benoxacor doses were selected to approximate the lifetime human exposure based on benoxacor levels reported in surface water (Woodward *et al.*, 2018). Each exposure group (0, 0.5, 5, and 50 mg/kg b.w. benoxacor) consisted of 8 mice (2 cages of 4 animals/cage). The individuals administering the benoxacor were blinded to the exposure groups. All gavage needles and syringes were sterilized by autoclave.

Animals were euthanized 24 h after the final dose by carbon dioxide (CO_2) asphyxiation, followed by the harvest of vital tissues. The IACUC of the University of Iowa approved all methods (protocol number: 0082057-001). Whole blood was obtained via cardiac puncture, immediately transferred to a MiniCollect serum separator (Greiner Bio-One, Kremsmunster, Austria), and kept on ice for a minimum of 30 min to allow the blood to clot. The serum was collected through centrifugation at 1503 g at 4°C for 20 min. Serum was transferred to 1.5-ml plastic tubes (Eppendorf North America, Canada) and stored at −80°C until further analysis. Liver tissue was excised, aliquoted, and stored in either TRIzol reagent (Life Technologies, Carlsbad, California) for RNA sequencing, 10% neutral buffered formalin (NBF) for pathology, or flash-frozen in liquid nitrogen for metabolomics and redox enzyme measurements. All liver samples were stored at −80°C until analysis. The intestine was divided into 4 sections (duodenum, jejunum, ileum, and colon), and sections were stored in neutral NBF for pathology. Colon and cecal contents were collected in 1.5-ml plastic tubes, immediately frozen on dry ice, and stored at −80°C.

Pathology. Hematoxylin and eosin (H&E) stained slides of liver and cross-sections of duodenum, jejunum, ileum, and colon were prepared by the University of Iowa Pathology Core (Iowa City, Iowa). Slides were submitted to the Iowa State Comparative Pathology Core (College of Veterinary Medicine, Iowa State University, Ames, Iowa) for microscopic evaluation. The slides were scored for inflammation/infiltrate, type of exudate/infiltrate, villus epithelial necrosis, villus epithelial hyperplasia, crypt necrosis, and crypt hyperplasia by an American College of Veterinary Pathologists certified veterinary pathologist blinded to the exposure groups.

Bacterial 16S rRNA analysis. Microbiome analysis was done as previously published (Shahi *et al.*, 2019). Briefly, DNA was extracted from cecal contents from individual mice with a DNeasy PowerLyzer PowerSoil Kit (Qiagen, Hilden, Germany).

Bacterial 16s rRNA region V3–V4 was amplified (PCR primer sequences: forward 5' TCGTCGGCAGCGTCAGATGTGTATAAGA GACAGCCTACGGGNGGCWGCAG-3'; reverse 5'- GTCTCGTGGG CTCGGAGATGTGTATAAGAGACAGGACTACHVGGGTATCTAATC C-3'), samples were individually barcoded with the Nextera XT Index Kit (Illumina, San Diego, California), and the resulting PCR products were purified and sequenced with Illumina MiSeq. The sequence data have been uploaded to the Sequence Read Archive (https://www.ncbi.nlm.nih.gov/sra; last accessed December 2, 2021) under the BioProject ID PRJNA739368 and are freely accessible.

The Divisive Amplicon Denoising Algorithm 2 (DADA2) package version 1.18 in R was used to process sequencing data, and the Silva reference database (version 138.1) was used to map reads onto previously established taxa information. There was a total of 1,086,657 reads with an average read count of 36,221 per sample. Subsequent statistical analyses were performed utilizing R. α-Diversity was performed on preprocessed data as it looks at raw feature count. The data were then normalized by sum scaling to 1e−6 and generalized log transformation (base 10). This type of normalization was utilized as microbiome abundance data are zero-inflated and not normally distributed. Then the data were filtered to remove features with prevalence < 1 and/or relative abundance of < 1e−4. This filtering was applied to avoid identifying significant features absent in 1 group and minimally present in another. After normalization and filtering, 86 genera remained for analysis.

α-Diversity was performed using the Shannon and Chao-1 index. β-Diversity was assessed using the Weighted Unifrac distance metric. This metric was chosen because it looks at the quantity of each feature present and considers the phylogeny of these features in the group comparison. We used negative binomial regression for the bacterial count data. The log-transformed sample-specific total bacterial counts is used as the offset in order to correct for the variation in the total bacterial counts across samples. This model is more flexible than Poisson regression for zero-inflated data and is a major method for modeling microbiome data where zero inflation is common. We tested whether a bacterium is differentially expressed (DE) among the 4 groups: control, 0.5, 5, and 50 mg/kg b.w. We also tested whether the 3 exposure groups, that is, 0.5, 5, and 50 mg/kg b.w., are different from the control group. The Dunnett test was used to adjust the *p*-values for multiple testing as the 3 exposure groups are compared with the same control (Supplementary Table 1).

Liver transcriptomics. Total RNA was isolated from the liver using the GenElute Mammalian Total RNA Miniprep Kit per the manufacturer's protocol (Sigma-Aldrich). RNA concentration was quantified using a NanoDrop 2000 spectrophotometer (ThermoScientific, Waltham, Massachusetts) at a wavelength of 260 nm. Samples were sent to Novogene (Tianjin, China) for integrity evaluation and mRNA sequencing (RNA-seq). The raw and analyzed RNA-seq data were deposited into the NCBI GEO database (GSE172173).

FASTQ paired-end read data were processed by the "bcbio-nextgen.py" (v.1.2.2) pipeline running in "RNA-seq" mode (https://github.com/chapmanb/bcbio-nextgen; last accessed December 2, 2021) on the University of Iowa's ARGON HPC cluster (Guimera, 2012). The pipeline performs quality control (QC), alignment, and quantification. QC was carried out using "FastQC" (v.0.11.8; https://www.bioinformatics.babraham.ac.uk/projects/fastqc/; last accessed December 2, 2021) and "Qualimap" (v.2.2.2) to examine the BAM alignments and provide an overview

of common problems (García-Alcalde *et al.*, 2012; Okonechnikov *et al.*, 2016). The reference genome used for alignment and quantification was Ensembl's "mm10." All samples passed basic QC checks. All samples had > 30M reads/sample as recommended by the ENCODE consortium, and all samples had mapping rates to the reference genome > 88% and exonic mapping rates > 70%. The "hisat2" (v.2.2.0) aligner was used for read mapping, and "salmon" aligner (v1.1.0) was used for rapid alignment-free quantification (Bray *et al.*, 2016; Kim *et al.*, 2015). The R package "tximport" (v.1.12.3) was used to import salmon's transcript-level quantifications and summarize to estimated counts at the gene level for DE gene analysis that was performed using the "DESeq2" (v.1.24.0) package in R (v.3.6.1) (Love *et al.*, 2014; Soneson *et al.*, 2015). Genes were considered DE if they had an FDR-adjusted *p*-value < .1. To correct for poor clustering in the PCA analysis, we performed surrogate variable analysis (SVA) analysis using the "sva" package (v.3.32.1). Assuming 2 hidden batch variables, we found that SV1 and SV2 correlated strongly with PC2 and PC1, respectively (whereas benoxacor dose did not correlate with either PC). We found 163 DEGs using the DESeq2 implementation of the "likelihood ratio test" (full-model design $\sim$ batch + dose + SV1+SV2; reduced model $\sim$ batch + SV1+SV2). DEGs were analyzed using iPathwayGuide (Advaita Bioinformatics, https://www.advaitabio.com/ipathwayguide; last accessed December 2, 2021) to detect and predict significantly impacted pathways, biological processes, and molecular interactions. These analyses implement an "Impact Analysis" approach, which considers the direction and type of all signals on a pathway along with the position, role, and type of each gene (Ahsan and Drăghici, 2017; Donato *et al.*, 2013; Draghici *et al.*, 2007; Tarca *et al.*, 2009).

Metabolomic analysis. Targeted metabolomic data were collected with a screening list containing 361 metabolites following protein precipitation with methanol at the Northwest Metabolomics Research Center (University of Washington, Seattle, Washington) in liver and serum following published procedures (Miklas *et al.*, 2019). Briefly, samples were extracted and analyzed in the multiple-reaction-monitoring mode on XBridge BEH Amide XP columns (Waters Technologies Corporation, Milford, Massachusetts) with an AB Sciex 6500+ Triple Quadrupole MS equipped with ESI ionization source in the ESI− and ESI+ ionization mode. In liver samples, 172 metabolites were measured, whereas 173 metabolites were quantified in the plasma samples. A pooled human serum sample was used to monitor system performance, and pooled study samples were used to monitor data reproducibility. Both sample batches (32 tissue and 32 plasma samples) generated reproducible data with an average coefficient of variances of 5.6%–6.9%. Generated MS data for the tissue samples were normalized versus BCA total protein count. The MS data for the plasma samples were not normalized. Metabolomics data for individual animals are openly available in Iowa Research Online at https://doi.org/10.25820/data.006157 (Simonsen and Lehmler, 2021).

Metabolites with > 50% missing values were removed from the subsequent data analysis. The remaining missing values were imputed with the one-half lowest intensity detected for that metabolite across all samples. Metabolites detected with relative standard deviation > 30% in multiple injected QC samples were removed from the datasets. As a result, 173 and 172 metabolites were included in the serum and liver data, respectively, for further processing. Data were normalized by the sum of total metabolite intensity (serum) or protein level (liver), and log2 transformed. Data variability and group clustering were visualized with score plots in principal component analyses. Further univariate analysis for selecting dose-dependent metabolites was performed with a linear regression model using *LinearModelFit* function in R package *NormalizeMets* (De Livera *et al.*, 2018) to generate raw *p* values reflecting the correlation between metabolite intensities and dose levels. Raw *p* values were adjusted for false discovery rate with Benjamini and Hochberg method (Benjamini and Hochberg, 1995). If applicable, analyses were performed with MetaboAnalyst 4.0 (Chong *et al.*, 2018) or R (version 3.6.3). Because only a limited number of metabolites (5% for serum data and 9% for liver data) were obtained with a raw *p*-value < .05, no further pathway analysis was performed.

Activity of antioxidant enzymes. Catalase activity was determined on whole mouse livers, homogenized in 50 mM potassium phosphate buffer (pH 7.8, with 1.34 mM diethylenetriaminepentaacetic acid) as described (Spitz *et al.*, 1990). Activity (expressed as mk units/mg of protein) was determined by measuring the disappearance of 10 mM hydrogen peroxide (240 nm) as previously reported (Ahmad *et al.*, 2005). Superoxide dismutase (SOD) activity was determined on mouse liver homogenates (as above) using an indirect competitive inhibition assay as described previously (Ahmad *et al.*, 2005; Spitz and Oberley, 1989). Glutathione peroxidase (GPx) activity was determined in mouse liver homogenates by monitoring NADPH oxidation in the presence of reduced glutathione (GSH) and glutathione reductase, using H_2O_2 as the substrate as previously reported (Owens *et al.*, 2012). Glutathione S-transferases (GSTs) activity was measured using 1 mM 1-chloro-2,4-dinitrobenzene as substrate (Simons and Vander Jagt, 1977). One unit of activity is defined as that amount of protein that catalyzes the formation of 1 μmol of thioether per minute and is expressed as munits per milligrams protein.

In vitro *metabolism of benoxacor.* The metabolism of benoxacor was studied in liver microsomes and cytosol from male mice (Simonsen *et al.*, 2020). Briefly, pooled microsomes from male C57BL/6 mice were incubated for up to 30-min at 37°C. Each incubation contained 5 μM benoxacor, 0.5 mM NADPH, 0.1 mg/ml microsomal protein, phosphate buffer (0.1 M, pH 7.4), and magnesium chloride (3 mM) in a total incubation volume of 5 ml. A 500 μl aliquot was taken every 5-min and quenched in ice-cold 1% formic acid. Cytosolic incubations were performed with 5 μM benoxacor, 5 mM GSH, and 0.1 mg/ml cytosolic protein, phosphate buffer (0.1 M, pH 7.4), and magnesium chloride (3 mM), also in a total incubation volume of 5 ml. A 500 μl aliquot was taken every 5-min and quenched in ice-cold 1% formic acid. All incubations were performed in triplicate.

Gas chromatographic analyses. We used an Agilent 6890 N gas chromatograph coupled to an Agilent 5975 MSD (GC/MS) (Agilent Technologies, Santa Clara, California) in the selected ion monitoring mode for the analysis of benoxacor (Simonsen *et al.*, 2020). Samples were injected in the splitless mode with an inlet temperature of 280°C and separated on an SLB-5MS column (30 m length, 0.25 mm inner diameter, 0.25 μm film thickness; Supelco, Bellefonte, Pennsylvania) with a constant helium flow rate of 1 ml/min. The oven parameters were set as follows: initial temperature, 50°C hold for 1 min, 15°C/min to 240°C, hold for 13 min, 15°C/min to 300°C, and hold for 10 min. The source and quadrupole temperatures of the mass selective detector were set at 230°C and 150°C, respectively.

For all enantioselective analyses, we used an Agilent 7890 A gas chromatograph coupled to a ^{63}Ni-μECD following our previous protocol (Simonsen *et al.*, 2020). We utilized a CP-Chiralsil DEX CB (CB) column (25 m length, 0.25 mm inner diameter, 0.25 μm film thickness; Agilent) for all enantiomeric fraction (EF) determinations using the following temperature settings: 50°C, hold for 1 min, 10°C/min to 145°C, hold for 50 min, 15°C/min to 200°C, hold for 12 min. The injector temperature was set at 250°C, and a constant helium flow rate of 2 ml/min was used. EF values were calculated by the equation:

$$EF = A1/(A1 + A2). \qquad (2)$$

A_1 and A_2 represent the areas of the first (E_1) and second (E_2) eluting enantiomer of benoxacor, respectively.

Quality assurance/quality control of benoxacor analyses. The following control incubations were performed in parallel with all experiments to ensure a rigorous study: Benoxacor spiked buffer to determine on-going recovery and precision, vehicle spiked (DMSO) buffer to assess matrix effects of the vehicle, benoxacor spiked microsomes, or cytosol without cofactor to determine contributions of enzymes (eg, carboxylesterases [CESs]) not requiring NADPH (microsomes) or GSH (cytosol), heat-inactivated microsomes or cytosol with the respective cofactors and benoxacor to study benoxacor loss by protein binding, and benoxacor spiked buffer containing NADPH or GSH to control for interactions of benoxacor with the cofactors.

The response of all compounds in the GC/MS analyses was linear at the concentrations analyzed in this study ($R^2 \geq 0.9983$). The limit of detection (LOD) was calculated using blank buffer samples ($n = 8$) following the IUPAC method (Mocak *et al.*, 1997) using the equation:

$$LOD = \text{mean blanks} + k * \text{Standard deviation of the blanks}, \qquad (3)$$

where k is Student's t value for a degree of freedom at a 99% confidence level of $n-1 = 7$. The LOD was calculated to be 2 ng. No loss of benoxacor was observed for spiked controls after correcting for the loss of the recovery standard (corrected benoxacor recovery = 100% ± 2%; $n = 12$). The recovery of trifluralin for all samples ranged from 80% to 105% and averaged 91% ± 6% ($n = 234$).

The resolution (R) of the enantiomers of benoxacor on the CB column was calculated by determining the difference of the enantiomer peak retention times divided by the average peak widths as:

$$R = \frac{t_{R2} - t_{R1}}{\frac{1}{2}(W_1 + W_2)}. \qquad (4)$$

Only analyses that had a baseline resolution ($R > 1$) were included in further analysis. Racemic benoxacor had an EF = 0.48 ± 0.01 ($n = 6$).

Estimation of intrinsic and scaled clearances. We calculated the apparent intrinsic clearance (CL_{int}) and the scaled intrinsic clearance (scaled CL_{int}) from the microsomal and cytosolic depletion experiments using a previously reported method (Houston and Galetin, 2008; Simonsen *et al.*, 2020). The initial rate of benoxacor depletion (k_{dep}) was calculated by linearizing the data through a natural logarithm transformation of the percentages of benoxacor depletion versus time. We then used linear regression to calculate when 50% of the benoxacor was depleted

(in vitro $t_{1/2}$). We used equation 5 to calculate the CL_{int}, where V is the incubation volume.

$$CL_{int} = \sum_i^n \left\langle \frac{V_{max, i}}{K_{mi}} \right\rangle = \frac{0.693 \times V}{\text{in vitro } t_{\frac{1}{2}}} \qquad (5)$$

Statistical analyses. Data are represented as the mean ± standard deviation. All statistical analyses for antioxidant enzyme assays and *in vitro* metabolism were performed on Graphpad Prism 9.0.0. One-way ANOVA was used to compare the activities of the redox enzymes across exposure groups and the 30-min time points in the *in vitro* metabolism studies. The ANOVA results were followed up with Tukey's test for multiple comparisons. All tests were considered significant at $p < .05$.

RESULTS

Analysis of ToxCast Data of Dichloroacetamide Safeners
We utilized ToxCast toxicity information to compare the potential toxicity of dichloroacetamide safeners to several of their coformulated herbicides (ie, metolachlor, acetochlor, and alachlor), the potential safener metabolite dichloroacetic acid, and 2 structurally unrelated pesticides, 2,4-D and dicamba, using the ToxPi tool. In the ToxPi analysis, benoxacor clustered with the herbicides acetochlor and alachlor (Figure 1), 2 herbicides more toxic than metolachlor (Dierickx, 1999; Kale *et al.*, 2008). The safeners dichlormid and AD-67 did not show much activity in these assays, suggesting that they are not as much of a toxicological concern as benoxacor. Furilazole, the other commercially available dichloroacetamide safener, did not have any available data. Dichloroacetic acid only had active hit calls for 7 of over 800 assays. This observation is interesting as dichloroacetic acid is known to cause immunotoxicity and hepatotoxicity (Cai *et al.*, 2007; Moser *et al.*, 1999). Like dichloroacetic acid, dicamba and 2,4-D had very little activity for the assays tested. This observation suggests that dichloroacetic acid, dicamba, and 2,4-D do not act the same way as chloroacetanilide herbicides and dichloroacetamide safeners.

Benoxacor was predicted to activate the farnesoid X receptor (FXR) and pregnane X receptor (PXR), leading to hepatic steatosis (adverse outcome pathways [AOPs] 60 and 61, respectively) (Villeneuve *et al.*, 2014a,b; Vinken, 2013). Benoxacor was also predicted to inhibit aromatase leading to infertility (AOP 153) and activating ESR1 leading to breast cancer (AOP 200). Metolachlor, a well-documented hepatotoxicant (Dierickx, 1999; Hartnett *et al.*, 2013; Kale *et al.*, 2008), was also predicted to affect the same AOPs similarly to benoxacor. These results suggest that benoxacor, like the hepatotoxic herbicides, may cause hepatotoxicity in mammals by mechanisms involving the activation of nuclear transcription factors, such as PXR and FXR. Based on the analysis of the ToxCast data (Figure 1), we tested the hypothesis that subacute oral exposure of male mice to benoxacor causes hepatotoxicity.

Subacute Toxicity of Benoxacor in Mice
Body and organ weights. Organ weight changes have long been accepted as toxicological endpoints (Heywood, 1981; Michael *et al.*, 2007). Following a 3-day exposure to benoxacor, the body weight and the bodyweight-adjusted weights of the spleen, kidneys, or brain were not significantly different between the exposure groups (Figs. 2A–D). The bodyweight-adjusted liver weight was significantly increased in the 50 mg/kg b.w. exposure group
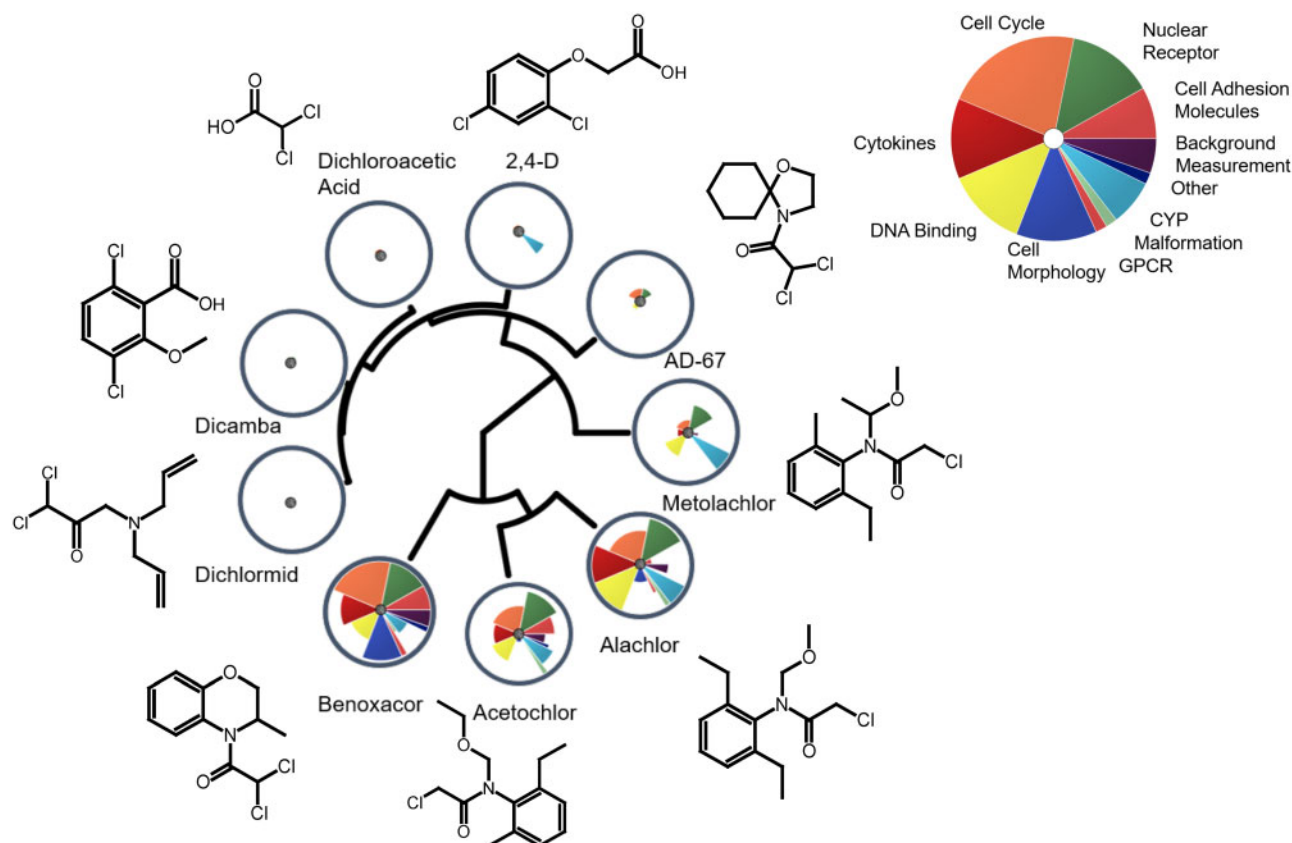
Figure 1. Benoxacor's ToxCast profile clusters with the chloroacetanilide herbicides acetochlor and alachlor in ToxPi hierarchical clustering. The distance that an arc extends is proportional to the relative evidence of concern for each group of tests. Benoxacor represents the chemical of greatest concern under the testing parameters. The dark middle represents the percentage of missing data for each chemical.

($p = .0059$) (Figure 2E). The bodyweight-adjusted testes weight was also significantly increased in the 50 mg/kg b.w. exposure group ($p = .0152$) (Figure 2F).

Pathology. The intestines of male mice exposed to benoxacor showed no significant pathological changes compared with the control animals, irrespective of the dose. Six mice had multifocal to diffuse accumulation of lymphocytes and plasma cells in the duodenum or colon, but these were considered background findings. The liver also showed no significant differences between control and exposed animals. The livers of 14 mice, including 2 controls, had 1–3 mild foci of extramedullary hematopoiesis. No other effects were seen with H&E staining.

Bacterial 16S rRNA. Dose-dependent changes in the cecal microbiome following oral exposure to benoxacor were assessed using 16s rRNA analysis. To look at the overall microbial community structure, we analyzed both α- and β-diversity differences between the control and benoxacor groups. There was no significant difference in α-diversity between the control and benoxacor groups by the Chao1 ($p = .490$) or Shannon index ($p = .413$) (Supplementary Figure 1). β-Diversity was analyzed utilizing the Weighted Unifrac metric, and there was no significant difference in community structure between the control and benoxacor groups ($p = .877$).

We utilized negative binomial regression to compare individual genera differences between controls and exposure groups. We found 9 genera that showed an overall treatment effect and were significantly different between the control and 1 or more treatment groups, including *Pseudoscardovia*, *Dubosiella*, *Faecalibaculum*, *Clostridium sensu stricto 1*, *Defluviitaleaceae UCG-011*, *Butyricicoccus*, *Caproiciproducens*, *Romboutsia*, and *Parasutterella*. Benoxacor exposure showed a nonmonotonic dose effect on most genera with a significant treatment effect, as illustrated for selected genera in Figure 3. The most pronounced effect of benoxacor was observed on *Butyricicoccus*, which displayed an > 2-fold dose-dependent decrease in the normalized abundance. Overall, short-term exposure to benoxacor had minimal impact on the community structure of the gut microbiome of mice administered a range of benoxacor doses.

Transcriptomic analysis. RNA-seq analysis was performed to determine how subacute exposure to benoxacor alters the liver transcriptome. A total of 163 DE genes were seen out of the 10,130 genes measured for expression (Supplementary Table 2). DE genes included several xenobiotic processing genes, including *Cyp7a1*, *Cyp3a13*, and *Cyp26a1*. Other interesting genes that were DE include *Tifa*, *Mylk*, and *Cbs*. Several GO terms such as catabolic, cellular catabolic, and organic catabolic processes were significant in the iPathwayGuide impact analysis. The predicted upstream chemical analysis we performed allows for predicting chemicals that may be present within an experiment based on known interactions with gene expression. In our study, iPathwayGuide's upstream chemical analysis predicted that dichloroacetic acid, a putative intermediate metabolite of benoxacor, and the fungicide sedaxane induced gene expression patterns similar to benoxacor, sharing 15/16 and 15/21 consistent DE targets, respectively (Figure 4). However, they were not significant following multiple
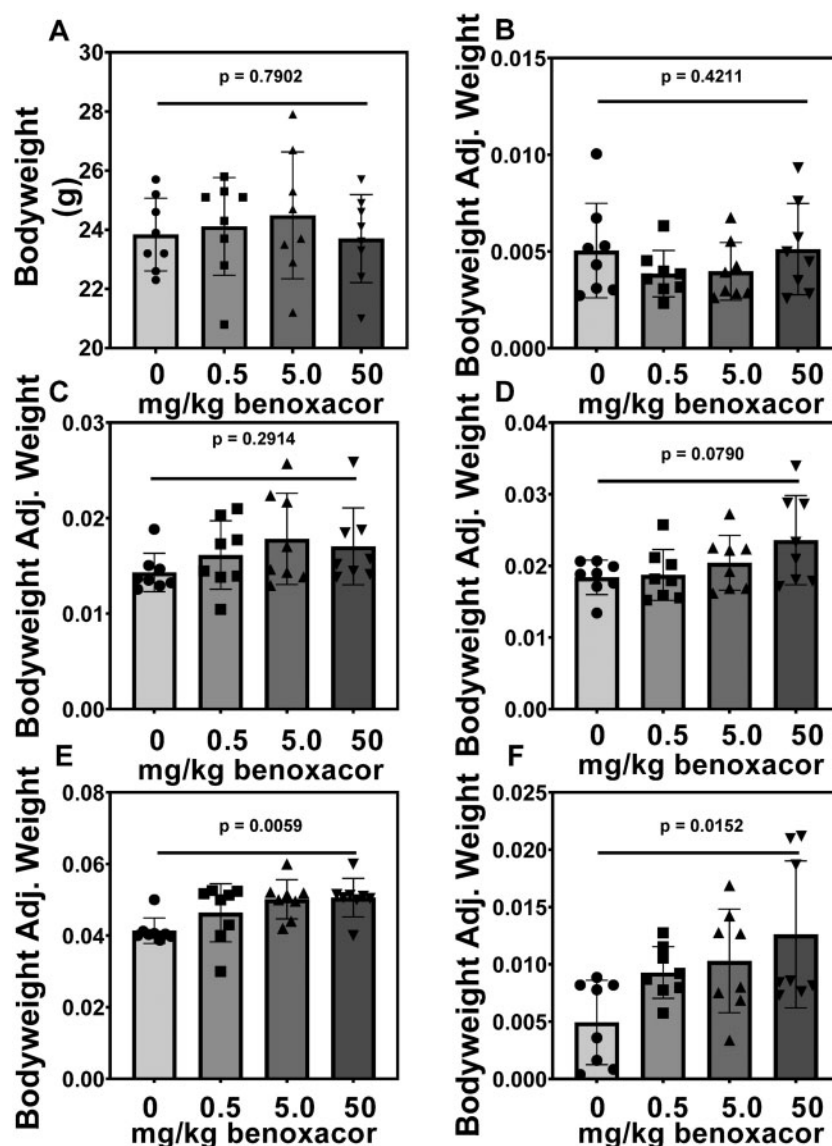
Figure 2. Benoxacor had limited effects on body weight and body weight-adjusted organ weight. A, Bodyweight was not significantly affected by benoxacor exposure. The bodyweight-adjusted weights: (B) spleen; (C) kidney; and (D) brain did not significantly change. Bodyweight-adjusted weights: (E) liver; (F) testes significantly increased in a dose-dependent manner. Data are reported as mean ± standard deviation. Significance was determined by 1-way ANOVA with Tukey's multiple comparisons test.

comparison corrections. Several pathways, including calcium signaling, protein processing in the endoplasmic reticulum, and metabolic pathways, were predicted to be affected by benoxacor exposure before correction for the false discovery rate.

Metabolomics. Targeted metabolomic analysis of serum and liver revealed that 9 of 172 and 15 of 172 metabolites were significantly altered by benoxacor exposure before correction for multiple comparisons (Supplementary Figs. 2–6 and Tables 3 and 4). In the serum, 6 of the 9 metabolites identified with the metabolomics analysis are associated with the pentose phosphate pathway. Levels of 2 metabolites associated with the gut microbiome, tryptamine, and deoxycholic acid (Bhattarai et al., 2018; Shi et al., 2021), appeared to be affected by benoxacor exposure. Adenylosuccinate, which is an intermediate in the interconversion between IMP and AMP (Meyer and Terjung, 1980), was identified along with acetylcarnitine, citrulline, lactate, and succinylcarnitine, metabolites associated with the TCA cycle (Huffman et al., 2014; Sahlin et al., 1990). Using

ANOVA, creatinine ($p = .0127$) and trigonelline ($p = .0494$) were significantly altered by benoxacor exposure in the liver (Supplementary Figure 4). The other changes in metabolite levels did not reach statistical significance after correcting for the false discovery rate with the Benjamini and Hochberg method and showed no clear dose-response relationship (Supplementary Figs. 2–6).

Activity of antioxidant enzymes. Exposure to metolachlor and related herbicides alters the activity of the antioxidant enzyme system in the rodent liver (Dierickx, 1999). Because of the similar effects of benoxacor and herbicides in the ToxPi analysis, the effect of benoxacor on the activity of catalase, GPx, GST, and SOD was assessed in the liver. The antioxidant enzymes catalase, GPx, and SOD showed no significant changes following the administration of benoxacor (Supplementary Figure 7). Furthermore, GSTs were not induced by exposure to benoxacor, unlike in maize (Fuerst et al., 1993) and Japanese carp (*Cyprinus carpio*) (Lay and Menn, 1987).
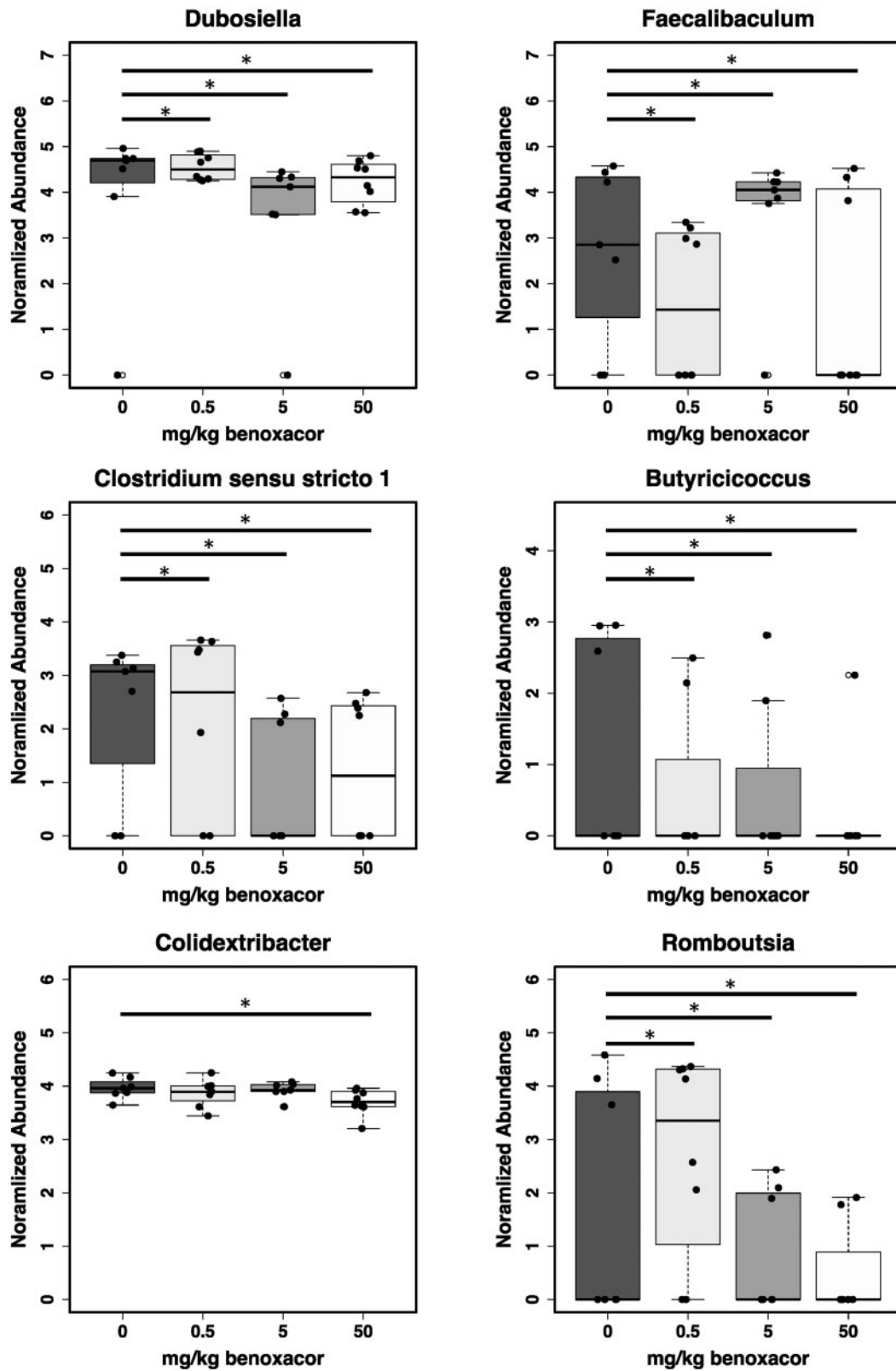
Figure 3. Differences in the levels of several bacteria in the cecum from mice exposed to different doses of benoxacor compared with vehicle only exposed mice, for example, *Pseudoscardovia, Dubosiella, Faecalibaculum, Clostridium sensu stricto 1, Defluviitaleaceae UCG-011, Butyricicoccus, Caproiciproducens, Romboutsia,* and *Parasutterella*. Negative binomial regression was used to analyze the bacterial count data for an exposure effect. The Dunnett test was used to adjust the *p*-values for multiple testing as the 3 exposure groups are compared with the same control. *p-value < .05.
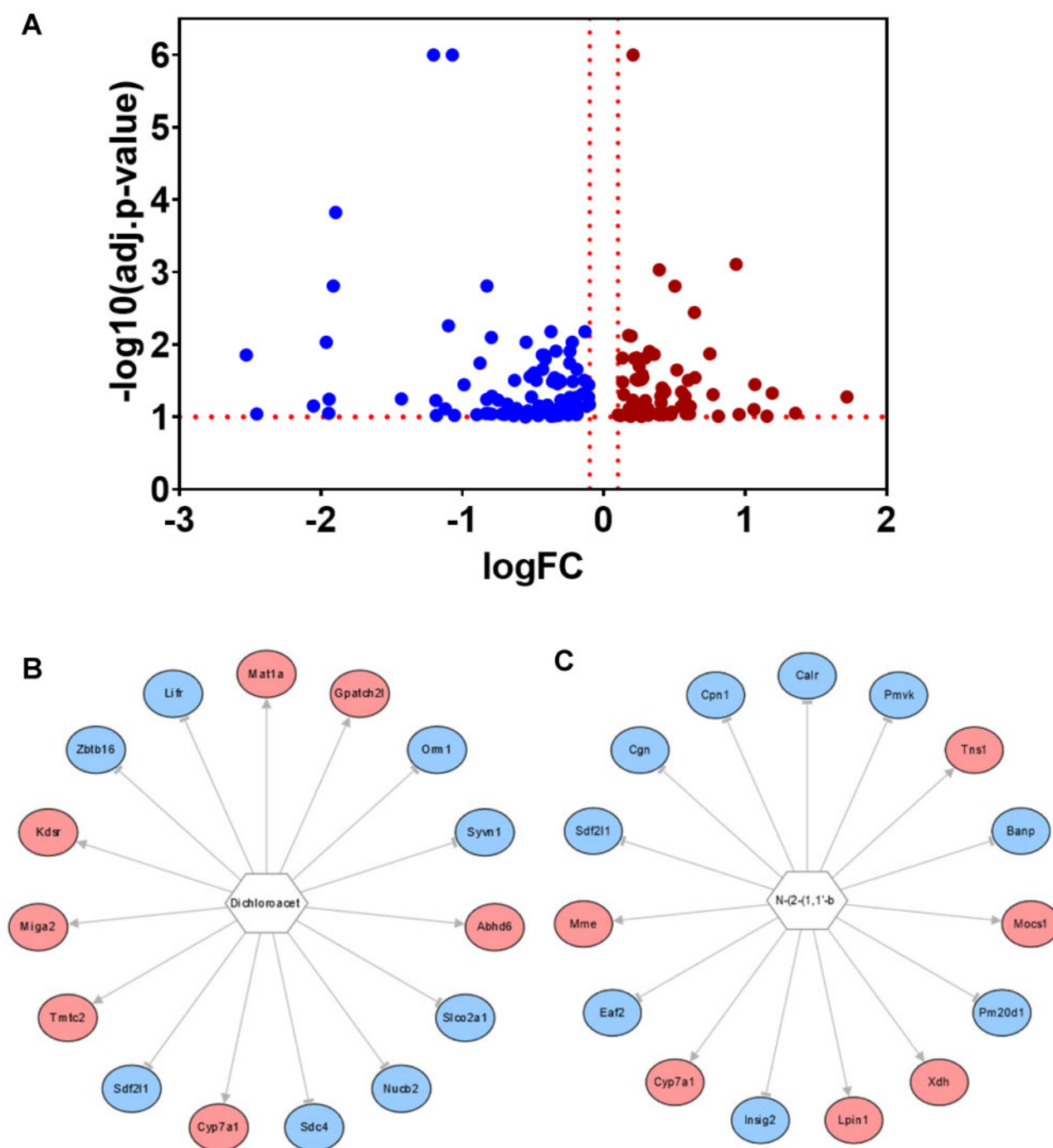
Figure 4. A, Volcano plot of differentially expressed genes from benoxacor exposure. Gene regulation profiles of DE genes resemble the regulation profiles of dichloroacetic acid (B) and the fungicide sexadane (C). Blue ovals indicate an increase in expression, and red ovals indicate decreased expression. Benoxacor and dichloroacetic acid regulate 15/21 genes (raw $p = .007$, $p = .889$) in the same manner. Benoxacor and sexadane regulate 15/16 DE genes (raw $p = .0001$, $p = .063$) in the same manner.

In Vitro Metabolism of Benoxacor in Mouse Microsomes and Cytosol

Safeners, such as benoxacor, induce metabolic enzymes, including cytochrome P450 enzymes (CYPs) and GSTs, to detoxify coformulated herbicides in plants (Jablonkai, 2013; Sivey et al., 2015). The same metabolic enzymes induced by safeners also lead to their metabolism in maize (Miller et al., 1996a,b). In rat

liver microsomes, benoxacor is metabolized by CYPs, with a minor contribution by CESs (Simonsen et al., 2020). Moreover, benoxacor is metabolized by cytosolic rat GSTs (Simonsen et al., 2020). Herein, we investigated the enantioselective metabolism of benoxacor using pooled microsomes and cytosol prepared from male mouse livers. The goal was to assess if the hepatic metabolism of benoxacor represents a (de-)toxication pathway.
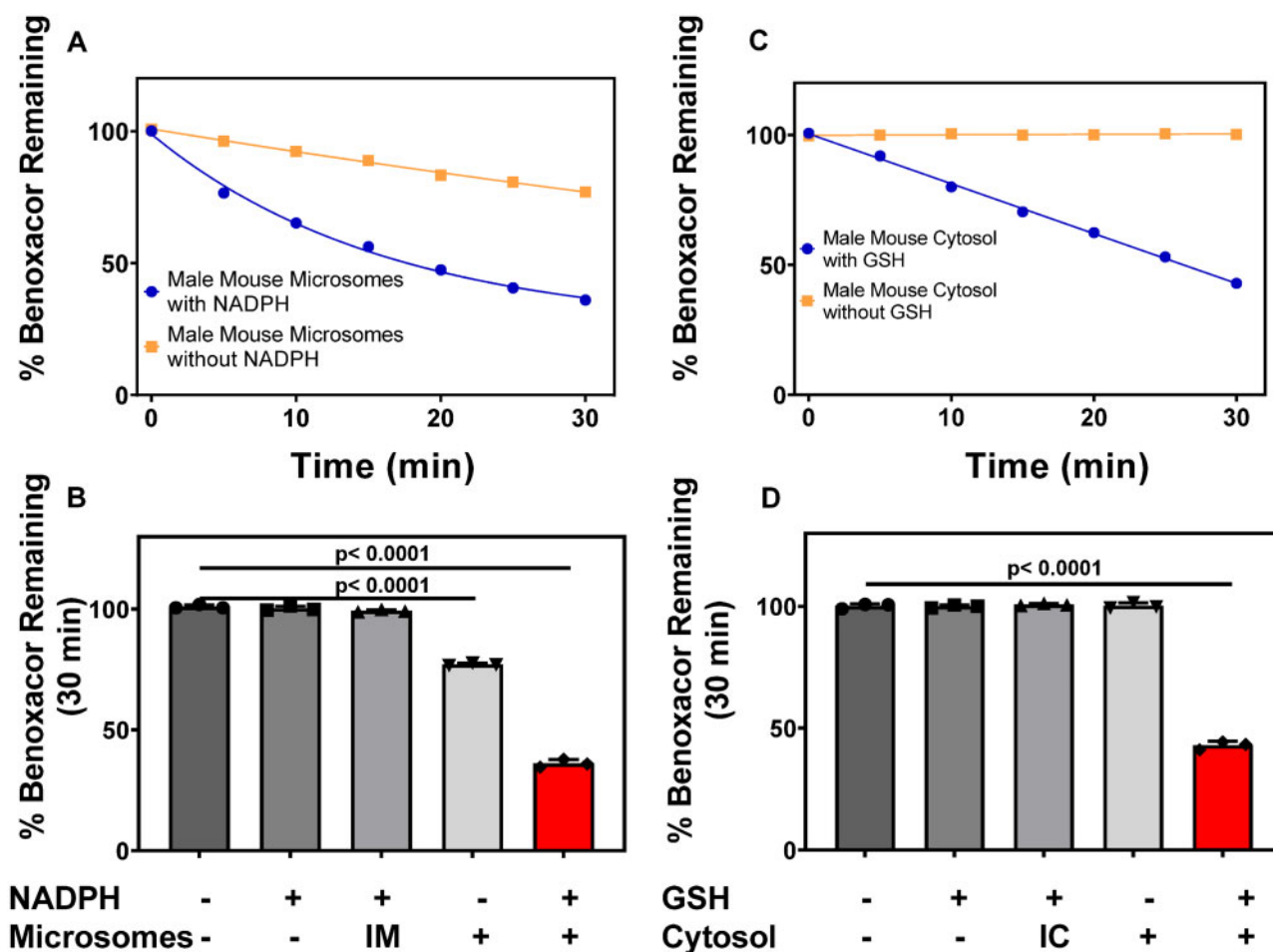
Figure 5. Benoxacor is depleted by CYPs and CESs in incubations with microsomes and GSTs in cytosol from mouse livers. A, Metabolism of benoxacor by microsomes with and without NADPH. B, The percentage of benoxacor in microsomal incubations from active and control incubations at 30 min; see text for more details. C, Metabolism of benoxacor by mouse cytosol with and without GSH. D, The percentage of benoxacor in cytosolic incubations from active and control incubations at 30 min; see text for more details. Data are reported as the mean ± standard deviation for 3 independent replicates; for some data points, the standard deviation is smaller than the size of the symbols. One-way ANOVA was used to determine significance in panels B&D with Tukey's multiple comparisons test. The percentages of benoxacor depletion are summarized in Supplementary Tables 5–7. NADPH, nicotinamide adenine dinucleotide phosphate; IM, heat-inactivated microsomes; GSH, glutathione.

Benoxacor metabolism by mouse liver microsomes in the presence of NADPH. Over a 30-min time-course, benoxacor was depleted in microsomes from male mouse livers in the presence of NADPH (Figure 5; Supplementary Table 5). Incubations were linear up to 5 min (Figure 5A). At 30 min, 36% ± 2% of benoxacor remained in experiments with NADPH and microsomes. Control incubations with heat-inactivated microsomes or without microsomes showed no disappearance of benoxacor (100% ± 1%) (Figure 5B). In microsomal incubations without NADPH, benoxacor was linearly depleted for the full 30-min incubation (Figure 5). With no NADPH present, 77% ± 1% of benoxacor remained after 30-min (Figure 5A; Supplementary Table 6).

Metabolism of benoxacor in mouse liver cytosol in the presence or absence of GSH. Benoxacor was also rapidly metabolized by mouse cytosol with the addition of GSH (Figure 5). At the 30-min time point, 43% ± 2% of benoxacor remained in incubations with cytosol from male mice (Figure 5C; Supplementary Table 7). When no GSH was added to the cytosol, there was no loss in benoxacor (100% ± 1%). Control incubations with heat-inactivated cytosol and without

cytosol showed no disappearance of benoxacor at 30 min (100% ± 1%) (Figure 5D).

Predicted intrinsic and scaled intrinsic clearance. Microsomal and cytosolic depletion experiments were used to estimate the metabolic clearance of benoxacor (Table 1). GSTs play the most extensive role in benoxacor clearance, but CYPs and CESs also
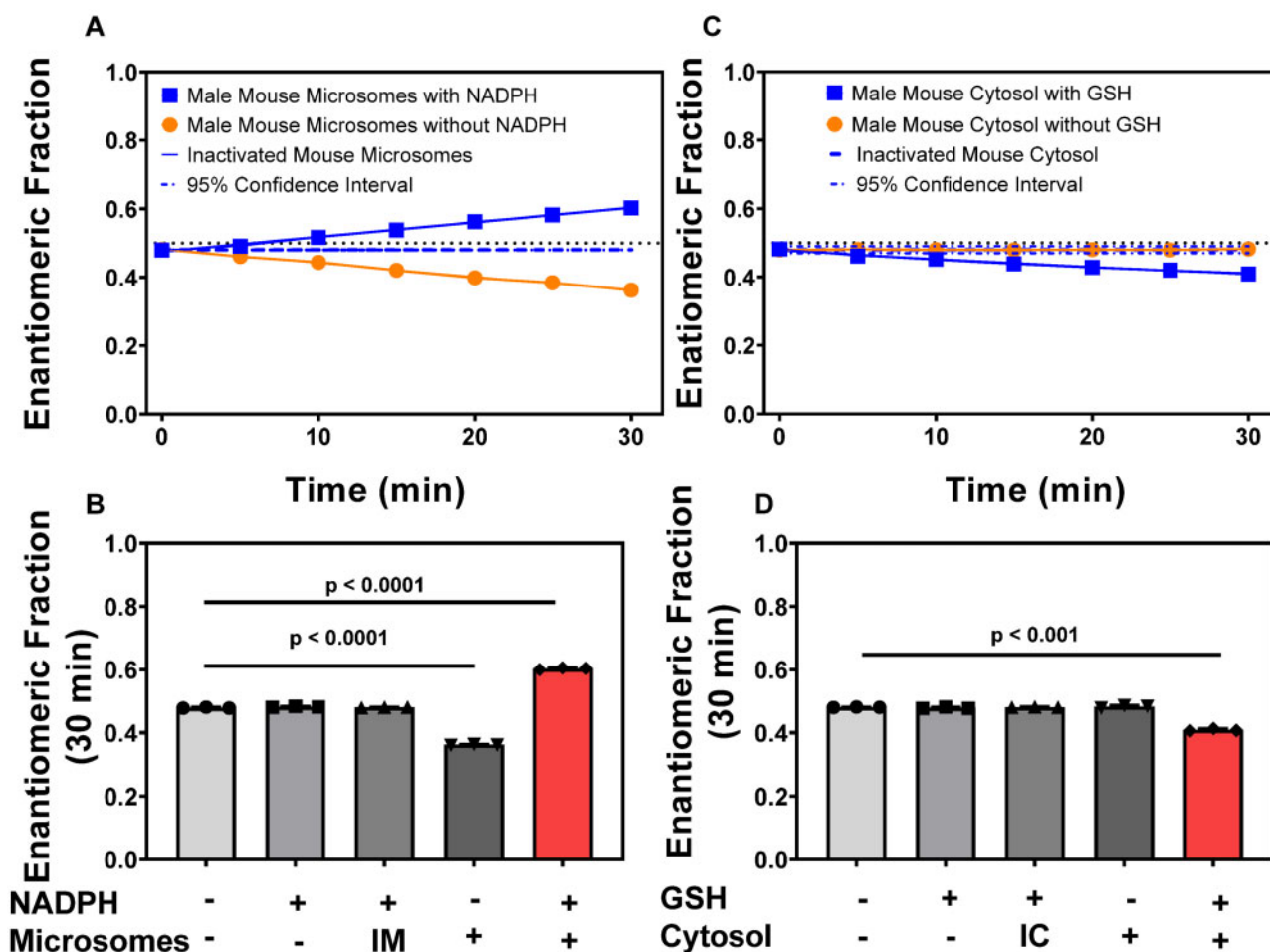
Table 1. Estimated Intrinsic and Scaled Intrinsic Clearance Values for CES, CYPs, and GSTs Estimated Based on a Previously Reported Method (Houston and Galetin, 2008)

Value	Male Mouse
Microsomal CES CL_{int} (ml/min/mg protein)	0.54
Microsomal CES scaled CL_{int} (ml/min/g liver)	20.77
Microsomal CYP CL_{int} (ml/min/mg protein)	1.05
Microsomal CYP scaled CL_{int} (ml/min/g liver)	40.22
Cytosolic CES CL_{int} (ml/min/mg protein)	N/A
Cytosolic CES Scaled CL_{int} (ml/min/g liver)	N/A
GST CL_{int} (ml/min/mg protein)	1.46
GST scaled CL_{int} (ml/min/g liver)	132.52

Figure 6. Benoxacor is enantioselectively metabolized in mouse liver microsomes and cytosol. A, Enantiomeric fraction change of benoxacor over time in 30-min incubations with microsomes prepared from male mouse livers. B, Enantiomeric fraction change at 30-min of active and control microsomal incubations; see text for more details. C, Enantiomeric fraction change of benoxacor over time in 30-min incubations with cytosol prepared from male mouse livers. D, Enantiomeric fraction change at 30-min of active and control cytosolic incubations; see text for more details. Data are the mean ± standard deviation for 3 independent replicates; for some data points, the standard deviation is smaller than the size of the symbols. Significance in panels B&D was determined with 1-way ANOVA with Tukey's multiple comparisons test. EF values are reported in Supplementary Tables 8–10. The dotted lines represent EF = 0.5. NADPH, nicotinamide adenine dinucleotide phosphate; IM, heat-inactivated microsomes.

contribute to the clearance of benoxacor in the mouse liver, with a rank order of GSTs > CYPs > microsomal CESs. Although the use of literature scaling factors and a lack of consideration of the role of transporters or the interplay of the enzymes in the liver represent limitations, these results provide insights that inform the interpretation of our *in vivo* studies.

Enantiomeric enrichment in microsomal incubations. CYPs enantioselectively metabolize environmentally relevant compounds, including pesticides (De Albuquerque *et al.*, 2018; Garrison, 2006; Zhang *et al.*, 2019). However, the enantioselective metabolism of safeners, like benoxacor, by mammalian CYPs and CESs has been mostly ignored. In experiments with microsomes from male mice with the addition of NADPH, there was enrichment of E_1-benoxacor (Figure 6A; Supplementary Table 8). The EF increased from 0.48 ± 0.01 to 0.60 ± 0.01 by the end of the 30-min incubation. When no NADPH was added to the microsomal incubations, there was enrichment of E_2-benoxacor (Figure 6A; Supplementary Table 9). Over the 30-min incubation the EF decreased from 0.48 ± 0.01 to 0.36 ± 0.01. This result suggests that CYPs predominantly metabolize E_2-benoxacor, and CESs predominantly metabolize E_1-benoxacor in the mouse liver.

Control incubations showed no change in EF compared with the EF of the racemic benoxacor used in the metabolism studies (Figure 6B).

Enantiomeric enrichment in cytosolic incubations with GSH. GSTs conjugate environmental contaminants and GSH in a stereospecific manner (Dostal *et al.*, 1988). When GSH was present within mouse cytosolic incubation, there was an enrichment of E_2-benoxacor (Figure 6C; Supplementary Table 10). Over the 30-min incubation, the EF decreased from 0.48 ± 0.01 to 0.41 ± 0.01. The EF remained racemic (EF = 0.48 ± 0.01) in incubations without GSH. No enantiomeric enrichment was seen in any control incubation (EF = 0.48 ± 0.01) (Figure 6D). This observation confirms that benoxacor depletion requires both mouse cytosol and GSH, consistent with the role of GSTs in the metabolism of benoxacor in the mouse liver.

DISCUSSION

Benoxacor was identified using ToxCast data as a safener that likely displays similar toxicities as alachlor and acetochlor, two well-studied hepatotoxicants. All 3 chemicals affect the

activation of the FXR and the PXR, key events associated with hepatic steatosis. Benoxacor is frequently coformulated with metolachlor (Sivey et al., 2015) and, as a result, is detected together with metolachlor in the environment (Woodward et al., 2018), thus raising concerns about human exposures to benoxacor and associated toxicities. In our animal study, we noted no significant effect of benoxacor exposure on body weight. This observation is not entirely surprising because the acute LD_{50} values of benoxacor are typically 2 orders of magnitude higher than the total dose used in the present study. However, we observed a statistically significant dose-dependent increase in liver weight. Similarly, oral benoxacor exposure led to increased liver and kidney weights at doses of > 40 mg/kg b.w./day in a chronic study in dogs (ECHA, nd). Consistent with similar mechanisms of toxicity, a dose-dependent increase in liver weight in rats was also seen after exposure of 30 days to acetochlor with significance reached at 500 mg/kg b.w./day (Song et al., 2019). However, following 15-day exposure to metolachlor, the liver weights of pregnant rats decreased at doses ≥ 300 mg/kg b.w./day (Tavares Vieira et al., 2016). Testes weights also increased in a dose-dependent fashion following benoxacor exposure. Similarly, other pesticides, including metolachlor, also target the testes (Mathias et al., 2012; Mehrpour et al., 2014).

Benoxacor exposure did not significantly alter bacterial richness (α-diversity) or overall bacterial community structure (β-diversity). However, benoxacor exposure affected the relative abundance of certain bacteria. For example, the relative abundance of *Butyricicoccus* decreased with increasing benoxacor dose. Interestingly, *Butyricicoccus* has been shown to be a beneficial bacterium with probiotic properties due to their ability to produce short-chain fatty acid butyrate (Geirnaert et al., 2014) and reduced in inflammatory disease such as inflammatory bowel disease (Eeckhaut et al., 2013). A nonmonotonic dose abundance relationship was observed for several other genera, including *Pseudoscardovia*, *Dubosiella*, *Faecalibaculum*, *Clostridium sensu stricto 1*, *Defluviitaleaceae UCG-011*, *Caproiciproducens*, *Romboutsia*, and *Parasutterella*. Changes in the abundance of bacteria, such as *Faecalibaculum* and *Clostridium*, has been linked to dysbiosis in several human disorders (Chen et al., 2020; Miquel et al., 2013). Several human microbiome studies show alteration of specific bacterial communities between disease and healthy state despite no difference in α- or β-diversity (Abe et al., 2020; Shahi et al., 2017). Thus, our microbiome data suggest that Benaoxacor might affect gut microbiota composition with depletion of beneficial bacteria.

RNA-seq analysis revealed only minor changes in the liver transcriptome of benoxacor exposed mice. *Cyp7a1* expression was significantly increased in the liver of exposed animals, which may affect bile acid and indole metabolite production; however, these changes in the expression of *Cyp7a1* were not reflected in the liver or serum metabolome. *Cyp7a1* is regulated by LXRα and FXR and is the mediator of the rate-limiting step in bile acid synthesis. Although this observation suggests that benoxacor may alter the gut liver axis, FXR, and PXR were not DE between the control and exposed groups. This finding contrasts the ToxCast data and likely results from species differences in FXR- and PXR-mediated regulation by bile acids (Lecluyse, 2001; Wang et al., 2006).

Although not statistically significant after adjusting for multiple comparisons, dichloroacetic acid was predicted by the iPathwayGuide analysis as 1 chemical that may have influenced gene expression in our experiment, owing to a profile of known DE genes that share a high degree of overlap with the measured DEGs following benoxacor treatment. Although the metabolites of benoxacor in mice and other mammalian species are currently unknown, dichloroacetic acid is a likely metabolite formed by hydrolysis of the amide group of benoxacor, as indirectly suggested by our metabolism study with rat liver subcellular fractions (Simonsen et al., 2020). Dichloroacetic acid is a well-known disinfection by-product with a maximum contaminant level of 60 μg/l established by the U.S. EPA (Villanueva and Argente, 2014; Villanueva et al., 2018). Dichloroacetic acid is a liver carcinogen in mice that causes dysregulation of oxidative metabolism and alters lipid and glucose homeostasis through acetyl coenzyme A (Ac-CoA) (Wehmas et al., 2017). However, in the ToxCast analysis, dichloroacetic acid only tested positive in 7 of over 800 high-throughput tests, highlighting why relying on high-throughput assays can be misleading. The fungicide sedaxane, a statistically significant chemical identified in the iPathwayGuide analysis, had a nearly identical profile to what was seen with benoxacor exposure. Sedaxane has been shown to increase embryonic development in zebrafish (Yao et al., 2018). However, the mammalian toxicity of this fungicide is poorly investigated.

The metabolomics results identified changes in 6 serum metabolites associated with the pentose phosphate pathway following benoxacor exposure. Benoxacor exposure appeared to affect levels of metabolites associated with intracellular energy homeostasis and the tricarboxylic acid (TCA) cycle in the liver (Hui et al., 2017; Indiveri et al., 2011; Tao et al., 2020). These changes were not statistically significant; however, it is noteworthy that similar effects on the liver metabolome were seen in rats following a 12-week exposure to other chlorinated disinfection by-products present in swimming pools (Li et al., 2015). An increase in metabolites in the pentose phosphate pathway and TCA cycle is consistent with an involvement of dichloroacetic acid, which acts as a pyruvate analog to inhibit pyruvate dehydrogenase kinase, thus reducing glycolysis and leading to an uptake of glucose into the mitochondria within the TCA cycle (Schwartz et al., 2017; Stacpoole et al., 2008; Wehmas et al., 2017). The uptake of glucose results in the activation of the pentose phosphate pathway, causing an increase in ribose-5-phosphate and a shift toward anabolic ATP production (Schwartz et al., 2017; Vander Heiden et al., 2009). The reason for only seeing marginal effects in this study is likely due to the much lower doses used compared with earlier studies with dichloroacetic acid and other disinfection by-products (Wehmas et al., 2017). For example, the EPA has established a NOAEL of 150 mg/kg-day in rats following a 14-day exposure to cause these effects (EPA, 2003). Additional studies are needed to confirm that dichloroacetic acid is indeed a mouse metabolite of benoxacor.

The levels and activities of liver antioxidant enzymes are frequently altered by pesticide exposure (Huang et al., 2020; Ojha et al., 2011; Rezg et al., 2008). In the present study, benoxacor did not exhibit any significant effects on the activity of antioxidant enzymes within the liver. Similarly, acute intraperitoneal exposure of male mice to the dichloroacetamide safener dichlormid did not alter the GSH content in the liver, thus indicating that dichlormid did not alter the balance of the hepatic antioxidant system in mice (Lay and Casida, 1976). In contrast, oral exposure of carp to the dichloroacetamide safener dichlormid increased liver GSH content 2.1-fold (Lay and Menn, 1987). In plants, safeners protect crops against herbicide toxicity by inducing drug-metabolizing enzymes, including CYPs and GSTs, and their cosubstrates (Jablonkai, 2013). Thus, the induction of GSTs seems to be limited to plants (Fuerst et al., 1993) and fish (Lay and Menn, 1987), likely due to species differences between plants, fish, and mammals.

The modest effects of subacute exposure to benoxacor on the liver transcriptome and metabolome in male mice may be due to the rapid metabolism of benoxacor by hepatic CYPs, GSTs, and CESs, as previously seen with rat microsomes and cytosol (Simonsen et al., 2020). We tested this hypothesis in vitro and observed the rapid metabolism of benoxacor by microsomal and cytosolic enzymes, including CYPs and GSTs. Importantly, benoxacor undergoes hydrolysis by microsomal but not cytosolic CESs. Similarly, CESs play an albeit minor role in the hepatic metabolism of benoxacor in rats. In addition, benoxacor may be metabolized by CESs in other organs (eg, plasma CESs) and the gut microbiome. The gut microbiome is a "drug-metabolizing organ" that affects the oral bioavailability of many drugs and agrochemicals (Wilson and Nicholson, 2017). Although the metabolites of benoxacor have not been characterized to date, the evidence suggests that benoxacor undergoes rapid metabolism in mice and other mammals, yielding dichloroacetic acid as the ultimate toxicant. Future subchronic and chronic exposure studies are likely to yield more pronounced adverse effects at dose levels well below regulatory studies with benoxacor. Overall, a combination of high throughput screening data and in vitro metabolism are likely more effective at prioritizing "inert" ingredients for further toxicity.

SUPPLEMENTARY DATA

Supplementary data are available at Toxicological Sciences online.

DECLARATION OF CONFLICTING INTERESTS

The authors declared no potential conflicts of interest with respect to the research, authorship, and/or publication of this article.

ACKNOWLEDGMENTS

FUNDING

REFERENCES

Abe, K., Fujita, M., Hayashi, M., Okai, K., Takahashi, A., and Ohira, H. (2020). Gut and oral microbiota in autoimmune liver disease. Fukushima J. Med. Sci. 65, 71–75.

Ahmad, I. M., Aykin-Burns, N., Sim, J. E., Walsh, S. A., Higashikubo, R., Buettner, G. R., Venkataraman, S., Mackey, M. A., Flanagan, S. W., Oberley, L. W., et al. (2005). Mitochondrial $O_2^{-\bullet}$ and H_2O_2 mediate glucose deprivation-induced cytotoxicity and oxidative stress in human cancer cells. J. Biol. Chem. 280, 4254–4263.

Ahsan, S., and Drăghici, S. (2017). Identifying significantly impacted pathways and putative mechanisms with iPathwayGuide. Curr. Protoc. Bioinformatics 57, 57.15.1–57.15.30.

Benjamini, Y., and Hochberg, Y. (1995). Controlling the false discovery rate: A practical and powerful approach to multiple testing. J. R. Stat. Soc. Series B Stat. Methodol. 57, 289–300.

Bergeson, L. L. (2000). FIFRA: Federal Insecticide, Fungicide, and Rodenticide Act, Basic Practice Series. American Bar Association.

Bhattarai, Y., Williams, B. B., Battaglioli, E. J., Whitaker, W. R., Till, L., Grover, M., Linden, D. R., Akiba, Y., Kandimalla, K. K., Zachos, N. C., et al. (2018). Gut microbiota-produced tryptamine activates an epithelial G-protein-coupled receptor to increase colonic secretion. Cell Host Microbe 23, 775–785.e5.

Bolognesi, C., Bonatti, S., Degan, P., Gallerani, E., Peluso, M., Rabboni, R., Roggieri, P., and Abbondandolo, A. (1997). Genotoxic activity of glyphosate and its technical formulation roundup. J. Agric. Food Chem. 45, 1957–1962.

Bray, N. L., Pimentel, H., Melsted, P., and Pachter, L. (2016). Near-optimal probabilistic RNA-seq quantification. Nat. Biotechnol. 34, 525–527.

Byer, J. D., Struger, J., Sverko, E., Klawunn, P., and Todd, A. (2011). Spatial and seasonal variations in atrazine and metolachlor surface water concentrations in Ontario (Canada) using ELISA. Chemosphere 82, 1155–1160.

Cai, P., Boor, P. J., Khan, M. F., Kaphalia, B. S., Ansari, G. A. S., and König, R. (2007). Immuno- and hepato-toxicity of dichloroacetic acid in $MRL^{+/+}$ and $B_6C_3F_1$ Mice. J. Immunotoxicol. 4, 107–115.

Carvalho, F. P. (2017). Pesticides, environment, and food safety. Food Energy Secur. 6, 48–60.

Chen, D., Jin, D., Huang, S., Wu, J., Xu, M., Liu, T., Dong, W., Liu, X., Wang, S., Zhong, W., et al. (2020). Clostridium butyricum, a butyrate-producing probiotic, inhibits intestinal tumor development through modulating Wnt signaling and gut microbiota. Cancer Lett. 469, 456–467.

Cheng, S. L., Li, X., Lehmler, H.-J., Phillips, B., Shen, D., and Cui, J. Y. (2018). Gut microbiota modulates interactions between polychlorinated biphenyls and bile acid homeostasis. Toxicol. Sci. 166, 269–287.

Chong, J., Soufan, O., Li, C., Caraus, I., Li, S., Bourque, G., Wishart, D. S., and Xia, J. (2018). MetaboAnalyst 4.0: Towards more transparent and integrative metabolomics analysis. Nucleic Acids Res. 46, W486–W494.

Cox, C., and Surgan, M. (2006). Unidentified inert ingredients in pesticides: Implications for human and environmental health. Environ. Health Perspect. 114, 1803–1806.

De Albuquerque, N. C. P., Carrão, D. B., Habenschus, M. D., and De Oliveira, A. R. M. (2018). Metabolism studies of chiral pesticides: A critical review. J. Pharm. Biomed. Anal. 147, 89–109.

De Livera, A. M., Olshansky, G., Simpson, J. A., and Creek, D. J. (2018). NormalizeMets: Assessing, selecting and implementing statistical methods for normalizing metabolomics data. Metabolomics 14, 54.

Dierickx, P. (1999). Glutathione-dependent cytotoxicity of the chloroacetanilide herbicides alachlor, metolachlor, and propachlor in rat and human hepatoma-derived cultured cells. Cell. Biol. Toxicol. 15, 325–332.

Dix, D. J., Houck, K. A., Martin, M. T., Richard, A. M., Setzer, R. W., and Kavlock, R. J. (2007). The ToxCast program for prioritizing

toxicity testing of environmental chemicals. *Toxicol. Sci.* **95**, 5–12.

Donato, M., Xu, Z., Tomoiaga, A., Granneman, J. G., Mackenzie, R. G., Bao, R., Than, N. G., Westfall, P. H., Romero, R., and Draghici, S. (2013). Analysis and correction of crosstalk effects in pathway analysis. *Genome Res.* **23**, 1885–1893.

Dostal, L. A., Guthenberg, C., Mannervik, B., and Bend, J. (1988). Stereoselectivity and regioselectivity of purified human glutathione transferases pi, alpha-epsilon, and mu with alkene and polycyclic arene oxide substrates. *Drug Metab. Dispos.* **16**, 420–424.

Draghici, S., Khatri, P., Tarca, A. L., Amin, K., Done, A., Voichita, C., Georgescu, C., and Romero, R. (2007). A systems biology approach for pathway level analysis. *Genome Res.* **17**, 1537–1545.

ECHA. (nd). *2,2-Dichloro-1-(3-Methyl-2,3-Dihydro-4H-1,4-Benzoxazin-4-yl)Ethanone Repeated Dose Toxicity: Oral*. Available at: https://echa.europa.eu/registration-dossier/-/registered-dossier/28351/7/6/2. Accessed November 6, 2021.

Eeckhaut, V., Machiels, K., Perrier, C., Romero, C., Maes, S., Flahou, B., Steppe, M., Haesebrouck, F., Sas, B., Ducatelle, R., *et al.* (2013). *Butyricicoccus pullicaecorum* in inflammatory bowel disease. *Gut* **62**, 1745–1752.

EPA. (2003). *Toxicological Review of Dichloroacetic Acid*. Available at: https://cfpub.epa.gov/ncea/iris/iris_documents/documents/toxreviews/0654tr.pdf. Accessed November 6, 2021.

EPA. (nd). *TOXCAST: EPA ToxCast Screening Library*. Available at: https://comptox.epa.gov/dashboard/chemical_lists/TOXCAST. Accessed November 6, 2021.

Fuerst, E. P., Irzyk, G. P., and Miller, K. D. (1993). Partial characterization of glutathione S-transferase isozymes induced by the herbicide safener benoxacor in maize. *Plant Physiol.* **102**, 795–802.

García-Alcalde, F., Okonechnikov, K., Carbonell, J., Cruz, L. M., Götz, S., Tarazona, S., Dopazo, J., Meyer, T. F., and Conesa, A. (2012). Qualimap: Evaluating next-generation sequencing alignment data. *Bioinformatics* **28**, 2678–2679.

Garrison, A. W. (2006). Probing the enantioselectivity of chiral pesticides. *Environ. Sci. Technol.* **40**, 16–23.

Geirnaert, A., Steyaert, A., Eeckhaut, V., Debruyne, B., Arends, J. B., Van Immerseel, F., Boon, N., and Van de Wiele, T. (2014). *Butyricicoccus pullicaecorum*, a butyrate producer with probiotic potential, is intrinsically tolerant to stomach and small intestine conditions. *Anaerobe* **30**, 70–74.

Gianessi, L. P., and Reigner, N. P. (2007). The value of herbicides in US crop production. *Weed Technol.* **21**, 559–566.

Gray, M. E. (2002). Federal insecticide, fungicide, and rodenticide act. In *Encyclopedia of Pest Management* (D. Pimentel, Ed.), pp. 261–262. CRC Press, Boca Raton, FL.

Guimera, R. V. (2012). bcbio-nextgen: Automated, distributed next-gen sequencing pipeline. *EMBnet J.* **17**, 30.

Hartnett, S., Musah, S., and Dhanwada, K. R. (2013). Cellular effects of metolachlor exposure on human liver (HepG2) cells. *Chemosphere* **90**, 1258–1266.

Heywood, R. (1981). Target organ toxicity. *Toxicol. Lett.* **8**, 349–358.

Houston, J. B., and Galetin, A. (2008). Methods for predicting in vivo pharmacokinetics using data from in vitro assays. *Curr. Drug Metab.* **9**, 940–951.

Huang, T., Huang, Y., Huang, Y., Yang, Y., Zhao, Y., and Martyniuk, C. J. (2020). Toxicity assessment of the herbicide acetochlor in the human liver carcinoma (HepG2) cell line. *Chemosphere* **243**, 125345.

Huffman, K. M., Koves, T. R., Hubal, M. J., Abouassi, H., Beri, N., Bateman, L. A., Stevens, R. D., Ilkayeva, O. R., Hoffman, E. P.,

Muoio, D. M., *et al.* (2014). Metabolite signatures of exercise training in human skeletal muscle relate to mitochondrial remodelling and cardiometabolic fitness. *Diabetologia* **57**, 2282–2295.

Hui, S., Ghergurovich, J. M., Morscher, R. J., Jang, C., Teng, X., Lu, W., Esparza, L. A., Reya, T., Le, Z., Yanxiang Guo, J., *et al.* (2017). Glucose feeds the TCA cycle via circulating lactate. *Nature* **551**, 115–118.

Indiveri, C., Iacobazzi, V., Tonazzi, A., Giangregorio, N., Infantino, V., Convertini, P., Console, L., and Palmieri, F. (2011). The mitochondrial carnitine/acylcarnitine carrier: Function, structure and physiopathology. *Mol. Aspects Med.* **32**, 223–233.

Jablonkai, I. (2013). *Herbicide Safeners: Effective Tools to Improve Herbicide Selectivity*. In Herbicides - Current Research and Case Studies in Use (A. J. Price and J. A. Kelton, Eds.), IntechOpen, DOI: 10.5772/55168. Available at: https://www.intechopen.com/chapters/44977.

Kale, V. M., Miranda, S. R., Wilbanks, M. S., and Meyer, S. A. (2008). Comparative cytotoxicity of alachlor, acetochlor, and metolachlor herbicides in isolated rat and cryopreserved human hepatocytes. *J. Biochem. Mol. Toxicol.* **22**, 41–50.

Kim, D., Langmead, B., and Salzberg, S. L. (2015). HISAT: A fast spliced aligner with low memory requirements. *Nat. Methods* **12**, 357–360.

Koyama, K., Koyama, K., and Goto, K. (1997). Cardiovascular effects of a herbicide containing glufosinate and a surfactant: In vitro and in vivo analyses in rats. *Toxicol. Appl. Pharmacol.* **145**, 409–414.

Lari, S. Z., Khan, N. A., Gandhi, K. N., Meshram, T. S., and Thacker, N. P. (2014). Comparison of pesticide residues in surface water and ground water of agriculture intensive areas. *J. Environ. Health Sci. Eng.* **12**, 11.

Lay, M.-M., and Casida, J. E. (1976). Dichloroacetamide antidotes enhance thiocarbamate sulfoxide detoxification by elevating corn root glutathione content and glutathione S-transferase activity. *Pestic. Biochem. Physiol.* **6**, 442–456.

Lay, M. M., and Menn, J. J. (1987). Amelioration of toxicity of molinate to Japanese carp (*Cyprinus carpio*) with selected dichloroacetamides. *Pestic. Biochem. Physiol.* **28**, 149–154.

Lecluyse, E. L. (2001). Pregnane X receptor: Molecular basis for species differences in CYP3A induction by xenobiotics. *Chem. Biol. Interact.* **134**, 283–289.

Li, C. Y., Lee, S., Cade, S., Kuo, L.-J., Schultz, I. R., Bhatt, D. K., Prasad, B., Bammler, T. K., and Cui, J. Y. (2017). Novel interactions between gut microbiome and host drug-processing genes modify the hepatic metabolism of the environmental chemicals polybrominated diphenyl ethers. *Drug Metab. Dispos.* **45**, 1197–1214.

Li, J.-H., Wang, Z.-H., Zhu, X.-J., Deng, Z.-H., Cai, C.-X., Qiu, L.-Q., Chen, W., and Lin, Y.-J. (2015). Health effects from swimming training in chlorinated pools and the corresponding metabolic stress pathways. *PLoS One* **10**, e0119241.

Love, M. I., Huber, W., and Anders, S. (2014). Moderated estimation of fold change and dispersion for RNA-seq data with DESeq2. *Genome Biol.* **15**, 550.

Marvel, S. W., To, K., Grimm, F. A., Wright, F. A., Rusyn, I., and Reif, D. M. (2018). ToxPi Graphical User Interface 2.0: Dynamic exploration, visualization, and sharing of integrated data models. *BMC Bioinformatics* **19**, 80.

Mathias, F. T., Romano, R. M., Sleiman, H. K., de Oliveira, C. A., and Romano, M. A. (2012). Herbicide metolachlor causes changes in reproductive endocrinology of male Wistar rats. *ISRN Toxicol.* **2012**, 1–7.

Mehrpour, O., Karrari, P., Zamani, N., Tsatsakis, A. M., and Abdollahi, M. (2014). Occupational exposure to pesticides and consequences on male semen and fertility: A review. *Toxicol. Lett.* **230**, 146–156.

Meyer, R. A., and Terjung, R. L. (1980). AMP deamination and IMP reamination in working skeletal muscle. *Am. J. Physiol. Cell Physiol.* **239**, C32–C38.

Michael, B., Yano, B., Sellers, R. S., Perry, R., Morton, D., Roome, N., Johnson, J. K., Schafer, K., and Pitsch, S. (2007). Evaluation of organ weights for rodent and non-rodent toxicity studies: A review of regulatory guidelines and a survey of current practices. *Toxicol. Pathol.* **35**, 742–750.

Miklas, J. W., Clark, E., Levy, S., Detraux, D., Leonard, A., Beussman, K., Showalter, M. R., Smith, A. T., Hofsteen, P., Yang, X., *et al.* (2019). TFPa/HADHA is required for fatty acid beta-oxidation and cardiolipin re-modeling in human cardiomyocytes. *Nat. Commun.* **10**, 4671.

Miller, K. D., Irzyk, G. P., Fuerst, E. P., McFarland, J. E., Barringer, M., Cruz, S., Eberle, W. J., and Föry, W. (1996a). Identification of metabolites of the herbicide safener benoxacor isolated from suspension-cultured *Zea mays* cells 3 and 24 h after treatment. *J. Agric. Food Chem.* **44**, 3335–3341.

Miller, K. D., Irzyk, G. P., Fuerst, E. P., McFarland, J. E., Barringer, M., Cruz, S., Eberle, W. J., and Föry, W. (1996b). Time course of benoxacor metabolism and identification of benoxacor metabolites isolated from suspension-cultured *Zea mays* cells 1 h after treatment. *J. Agric. Food Chem.* **44**, 3326–3334.

Miquel, S., Martin, R., Rossi, O., Bermudez-Humaran, L. G., Chatel, J. M., Sokol, H., Thomas, M., Wells, J. M., and Langella, P. (2013). *Faecalibacterium prausnitzii* and human intestinal health. *Curr. Opin. Microbiol.* **16**, 255–261.

Mocak, J., Bond, A. M., Mitchell, S., and Scollary, G. (1997). A statistical overview of standard (IUPAC and ACS) and new procedures for determining the limits of detection and quantification: Application to voltammetric and stripping techniques (technical report). *Pure Appl. Chem.* **69**, 297–328.

Moser, V. C., Phillips, P. M., McDaniel, K. L., and Macphail, R. C. (1999). Behavioral evaluation of the neurotoxicity produced by dichloroacetic acid in rats. *Neurotoxicol. Teratol.* **21**, 719–731.

Oakes, D. J., and Pollak, J. K. (1999). Effects of a herbicide formulation, Tordon 75D®, and its individual components on the oxidative functions of mitochondria. *Toxicology* **136**, 41–52.

Ojha, A., Yaduvanshi, S. K., and Srivastava, N. (2011). Effect of combined exposure of commonly used organophosphate pesticides on lipid peroxidation and antioxidant enzymes in rat tissues. *Pestic. Biochem. Physiol.* **99**, 148–156.

Okonechnikov, K., Conesa, A., and García-Alcalde, F. (2016). Qualimap 2: Advanced multi-sample quality control for high-throughput sequencing data. *Bioinformatics* **32**, 292–294.

Owens, K. M., Aykin-Burns, N., Dayal, D., Coleman, M. C., Domann, F. E., and Spitz, D. R. (2012). Genomic instability induced by mutant succinate dehydrogenase subunit D (SDHD) is mediated by $O_2^{\bullet-}$ and H_2O_2. *Free Radic. Biol. Med.* **52**, 160–166.

Popp, J., Pető, K., and Nagy, J. (2013). Pesticide productivity and food security. A review. *Agron. Sustain Dev.* **33**, 243–255.

Reemtsma, T., Alder, L., and Banasiak, U. (2013). Emerging pesticide metabolites in groundwater and surface water as determined by the application of a multimethod for 150 pesticide metabolites. *Water Res.* **47**, 5535–5545.

Reeves, W. R., McGuire, M. K., Stokes, M., and Vicini, J. L. (2019). Assessing the safety of pesticides in food: How current regulations protect human health. *Adv. Nutr.* **10**, 80–88.

Rezg, R., Mornagui, B., El-Fazaa, S., and Gharbi, N. (2008). Biochemical evaluation of hepatic damage in subchronic exposure to malathion in rats: Effect on superoxide dismutase and catalase activities using native PAGE. *C. R. Biol.* **331**, 655–662.

Rose, C. E., Coupe, R. H., Capel, P. D., and Webb, R. M. T. (2018). Holistic assessment of occurrence and fate of metolachlor within environmental compartments of agricultural watersheds. *Sci. Total Environ.* **612**, 708–719.

Roubeix, V., Fauvelle, V., Tison-Rosebery, J., Mazzella, N., Coste, M., and Delmas, F. (2012). Assessing the impact of chloroacetanilide herbicides and their metabolites on periphyton in the Leyre River (SW France) via short term growth inhibition tests on autochthonous diatoms. *J. Environ. Monit.* **14**, 1655–1663.

Sahlin, K., Katz, A., and Broberg, S. (1990). Tricarboxylic acid cycle intermediates in human muscle during prolonged exercise. *Am. J. Physiol. Cell Physiol.* **259**, C834–C841.

Schwartz, L., Seyfried, T., Alfarouk, K. O., Da Veiga Moreira, J., and Fais, S. (2017). Out of Warburg effect: An effective cancer treatment targeting the tumor specific metabolism and dysregulated pH. *Semin. Cancer Biol.* **43**, 134–138.

Shahi, S. K., Freedman, S. N., and Mangalam, A. K. (2017). Gut microbiome in multiple sclerosis: The players involved and the roles they play. *Gut Microbes* **8**, 607–615.

Shahi, S. K., Zarei, K., Guseva, N. V., and Mangalam, A. K. (2019). Microbiota analysis using two-step PCR and next-generation 16S rRNA gene sequencing. *J. Vis. Exp.* (152), e59980.

Sharma, A., Kumar, V., Shahzad, B., Tanveer, M., Sidhu, G. P. S., Handa, N., Kohli, S. K., Yadav, P., Bali, A. S., Parihar, R. D., *et al.* (2019). Worldwide pesticide usage and its impacts on ecosystem. *SN Appl. Sci.* **1**, 1446.

Shi, Z., Chen, G., Cao, Z., Wu, F., Lei, H., Chen, C., Song, Y., Liu, C., Li, J., Zhou, J., *et al.* (2021). Gut microbiota and its metabolite deoxycholic acid contribute to sucralose consumption-induced nonalcoholic fatty liver disease. *J. Agric. Food Chem.* **69**, 3982–3991.

Simons, P. C., and Vander Jagt, D. L. (1977). Purification of glutathione S-transferases from human liver by glutathione-affinity chromatography. *Anal. Biochem.* **82**, 334–341.

Simonsen, D., Cwiertny, D. M., and Lehmler, H.-J. (2020). Benoxacor is enantioselectively metabolized by rat liver subcellular fractions. *Chem. Biol. Interact.* **330**, 109247.

Simonsen, D., and Lehmler, H.-J. (2021). Metabolomics dataset for the effects of benoxacor on the liver and gut microbiome of C57BL/6 mice (dataset). doi:10.25820/data.006157.

Sivey, J. D., Lehmler, H.-J., Salice, C. J., Ricko, A. N., and Cwiertny, D. M. (2015). Environmental fate and effects of dichloroacetamide herbicide safeners: "Inert" yet biologically active agrochemical ingredients. *Environ. Sci. Technol. Lett.* **2**, 260–269.

Soneson, C., Love, M. I., and Robinson, M. D. (2015). Differential analyses for RNA-seq: Transcript-level estimates improve gene-level inferences. *F1000Research* **4**, 1521.

Song, X., Zhang, F., Chen, D., Bian, Q., Zhang, H., Liu, X., and Zhu, B. (2019). Study on systemic and reproductive toxicity of acetochlor in male mice. *Toxicol. Res.* **8**, 77–89.

Spitz, D. R., Elwell, J. H., Sun, Y., Oberley, L. W., Oberley, T. D., Sullivan, S. J., and Roberts, R. J. (1990). Oxygen toxicity in control and H_2O_2-resistant Chinese hamster fibroblast cell lines. *Arch. Biochem. Biophys.* **279**, 249–260.

Spitz, D. R., and Oberley, L. W. (1989). An assay for superoxide dismutase activity in mammalian tissue homogenates. *Anal. Biochem.* **179**, 8–18.

Stacpoole, P. W., Kurtz, T. L., Han, Z., and Langaee, T. (2008). Role of dichloroacetate in the treatment of genetic mitochondrial diseases. *Adv. Drug Deliv. Rev.* **60**, 1478–1487.

Su, L., Caywood, L. M., Sivey, J. D., and Dai, N. (2019). Sunlight photolysis of safener benoxacor and herbicide metolachlor as mixtures on simulated soil surfaces. *Environ. Sci. Technol.* **53**, 6784–6793.

Surgan, M., Condon, M., and Cox, C. (2010). Pesticide risk indicators: Unidentified inert ingredients compromise their integrity and utility. *Environ. Manage* **45**, 834–841.

Tao, T., He, T., Mao, H., Wu, X., and Liu, X. (2020). Non-targeted metabolomic profiling of coronary heart disease patients with Taohong Siwu decoction treatment. *Front. Pharmacol.* **11**, 651.

Tarca, A. L., Draghici, S., Khatri, P., Hassan, S. S., Mittal, P., Kim, J.-S., Kim, C. J., Kusanovic, J. P., and Romero, R. (2009). A novel signaling pathway impact analysis. *Bioinformatics* **25**, 75–82.

Tavares Vieira, K. C. D. M., Couto, J. C., Zanetti, E., Sanches Junior, J. M., and Favareto, A. P. A. (2016). Maternal and fetal toxicity of Wistar rats exposed to herbicide metolachlor. *Acta Sci. Biol. Sci.* **38**, 91.

Vander Heiden, M. G., Cantley, L. C., and Thompson, C. B. (2009). Understanding the Warburg effect: The metabolic requirements of cell proliferation. *Science* **324**, 1029–1033.

Villanueva, C., and Argente, J. (2014). Pathology or normal variant: What constitutes a delay in puberty? *Horm. Res. Paediatr.* **82**, 213–221.

Villanueva, C. M., Gracia-Lavedan, E., Julvez, J., Santa-Marina, L., Lertxundi, N., Ibarluzea, J., Llop, S., Ballester, F., Fernández-Somoano, A., Tardón, A., *et al.* (2018). Drinking water disinfection by-products during pregnancy and child neuropsychological development in the INMA Spanish cohort study. *Environ. Int.* **110**, 113–122.

Villeneuve, D. L., Crump, D., Garcia-Reyero, N., Hecker, M., Hutchinson, T. H., Lalone, C. A., Landesmann, B., Lettieri, T., Munn, S., Nepelska, M., *et al.* (2014a). Adverse outcome pathway (AOP) development I: Strategies and principles. *Toxicol. Sci.* **142**, 312–320.

Villeneuve, D. L., Crump, D., Garcia-Reyero, N., Hecker, M., Hutchinson, T. H., Lalone, C. A., Landesmann, B., Lettieri, T., Munn, S., Nepelska, M., *et al.* (2014b). Adverse outcome pathway development II: Best practices. *Toxicol. Sci.* **142**, 321–330.

Vinken, M. (2013). The adverse outcome pathway concept: A pragmatic tool in toxicology. *Toxicology* **312**, 158–165.

Wang, S., Lai, K., Moy, F. J., Bhat, A., Hartman, H. B., and Evans, M. J. (2006). The nuclear hormone receptor farnesoid X receptor (FXR) is activated by androsterone. *Endocrinology* **147**, 4025–4033.

Wauchope, R. D. (1978). The pesticide content of surface water draining from agricultural fields—A review. *J. Environ. Qual.* **7**, 459–472.

Wehmas, L. C., Deangelo, A. B., Hester, S. D., Chorley, B. N., Carswell, G., Olson, G. R., George, M. H., Carter, J. H., Eldridge, S. R., Fisher, A., *et al.* (2017). Metabolic disruption early in life is associated with latent carcinogenic activity of dichloroacetic acid in mice. *Toxicol. Sci.* **159**, 354–365.

Wilson, I. D., and Nicholson, J. K. (2017). Gut microbiome interactions with drug metabolism, efficacy, and toxicity. *Transl. Res.* **179**, 204–222.

Woodward, E. E., Hladik, M. L., and Kolpin, D. W. (2018). Occurrence of dichloroacetamide herbicide safeners and co-applied herbicides in midwestern US streams. *Environ. Sci. Technol. Lett.* **5**, 3–8.

Yao, H., Yu, J., Zhou, Y., Xiang, Q., and Xu, C. (2018). The embryonic developmental effect of sedaxane on zebrafish (*Danio rerio*). *Chemosphere* **197**, 299–305.

Zhang, Z., Gao, B., He, Z., Li, L., Shi, H., and Wang, M. (2019). Enantioselective metabolism of four chiral triazole fungicides in rat liver microsomes. *Chemosphere* **224**, 77–84.